

# Computer modeling of dynamic behavior of rocking wall structures including the impact-related effects

Advances in Structural Engineering  
2016, Vol. 19(8) 1245–1261  
© The Author(s) 2016  
Reprints and permissions:  
sagepub.co.uk/journalsPermissions.nav  
DOI: 10.1177/1369433216642057  
ase.sagepub.com



Irshad M Qureshi and Pennung Warnitchai

## Abstract

Precast post-tensioned concrete rocking wall system is an innovative damage avoidance structural system for seismic regions. Past experimental works on the dynamic performance of rocking walls have identified the presence of high-frequency acceleration spikes in both lateral and vertical directions during the impact of wall base with the foundation. These acceleration spikes, acting together, can cause shear slip at the wall–foundation connection. This study is focused on the development of a computer model that can predict these acceleration spikes along with the identification of their effects on the dynamic performance of rocking walls. For this purpose, impact phenomenon at the wall–foundation joint has been discussed in detail and some general guidelines are set for the two important parameters of impact or contact modeling named as contact stiffness and contact damping. The finite element numerical models, based on the proposed guidelines, are found to predict the overall dynamic behavior of rocking walls along with the acceleration spikes quite efficiently. The acceleration spikes are found to be dependent on the lateral velocity at impact and the initial contact stiffness. So a velocity-dependent energy dissipation device along with a soft contact is found to be suitable for reducing these effects.

## Keywords

acceleration spikes, contact, finite element modeling, rocking wall

## Introduction

In recent years, focus is increasing in developing the structural system that can not only withstand the high seismic force demand in the wake of a major seismic event but also can limit the structural and nonstructural damage to a minimum level. For this reason, various structural systems have been evolved in the recent past. One such system is the unbonded post-tensioned precast concrete wall system commonly referred as rocking wall structural system (Priestley et al., 1999). A rocking wall consists of vertically stacked precast concrete panels clamped by unbonded post-tensioning (PT) from the top of the wall to the foundation. Initial PT in the PT tendons along with the self-weight resists the lateral force demand, and once the lateral actions overcome the vertical forces, the wall starts to rock about its toes, commonly referred as “gap opening.” The gap opening at the wall base limits the seismic force demand by exhibiting a geometric nonlinearity similar to the material nonlinearity in conventional reinforced concrete (RC) shear walls due to plastic hinge formation. Rocking wall characterizes a non-linear elastic behavior as shown in Figure 1(a). Different displacement and velocity-dependent energy

dissipation (ED) devices have been used in the past (Belleri et al., 2014; Morgen and Kurama, 2008; Kurama, 2002; Marriott et al., 2008; Priestley et al., 1999; Restrepo and Rahman, 2007; Schoettler et al., 2009; Toranzo, 2002) to counter the inherent low ED capacity. A rocking wall with an ED mechanism is often termed as a hybrid wall and characterizes a typical flag-shaped hysteresis behavior. Figure 1(a) to (c) shows the hysteresis behavior of rocking wall, ED mechanism, and hybrid wall, respectively.

In recent years, a lot of work has been done to develop the rocking wall structural system as a resilient lateral force-resisting system for the building structures. Experimental and analytical investigation showed the excellent performance of rocking wall structures against seismic actions by exhibiting a large ductility capacity and a minimal structural damage,

---

Structural Engineering Department, Asian Institute of Technology,  
Pathum Thani, Thailand

## Corresponding author:

Irshad M Qureshi, Structural Engineering Department, Asian Institute of Technology, P.O. Box 4, Klong Luang, Pathumthani 12120, Thailand.  
Email: st107392@ait.asia; m.irshad84@gmail.com

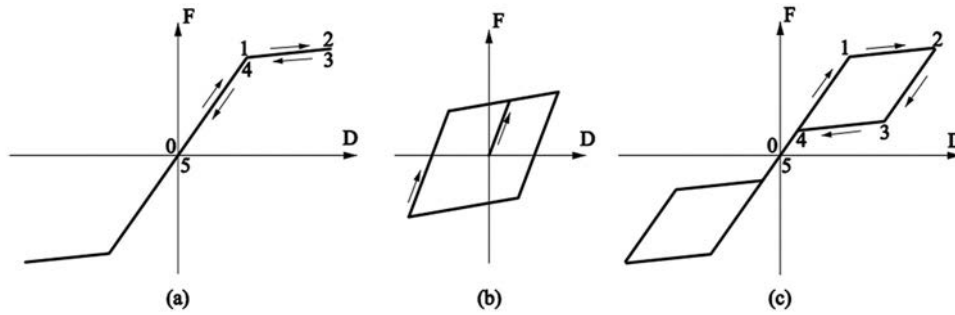


**Figure 1.** Idealized behavior of (a) rocking wall, (b) energy dissipation mechanism, and (c) hybrid wall.

strength degradation, and residual deformations. However, the majority of the work discussed the quasi-static response of rocking wall structures, and only a limited amount of experimental work has been conducted to investigate the dynamic performance of rocking walls (Belleri et al., 2014; Marriott et al., 2008; Schoettler et al., 2009; Toranzo, 2002; Wiebe and Christopoulos, 2010) resulting in a lack of model verification for the dynamic response. One of the conspicuous features of rocking wall seismic behavior is the presence of gap opening and closing phenomenon, characterized by an interaction of wall base and foundation top called as a contact. A short-duration, high-velocity contact in a dynamic domain called as an impact is found to induce short-duration large-amplitude accelerations, both in horizontal and vertical directions called as horizontal acceleration spikes (HASs) and vertical acceleration spikes (VASs), respectively, in the system response (Belleri et al., 2014; Marriott et al., 2008; Schoettler et al., 2009; Toranzo, 2002). Toranzo (2002) tested a three-story half-scale non-post-tensioned confined masonry rocking and hybrid walls on shake table and explicitly identified the presence of HAS and VAS in the experimental results. Belleri et al. (2014) tested a three-story half-scale rocking and hybrid wall on shake table, and the ratio of HAS and VAS to peak ground acceleration (PGA) for the maximum considered earthquake (MCE) level excitation was found to be approximately 4 and 7.5, respectively.

HAS phenomenon is not unique to the rocking wall dynamic behavior, but is also observed in the base isolation systems. It is attributed to a sharp change in lateral stiffness, at gap opening and closure, in a bilinear elastic hysteresis which is typical of a rocking wall behavior (Wiebe and Christopoulos, 2010). These acceleration spikes, observed with higher intensity near the rocking joint or in the lower stories, appear in the response for a very short interval of time and are generally out of phase with the displacement response. Wiebe and Christopoulos (2010) developed a closed-

form mathematical model for HAS and concluded that this effect is more intense when the change in stiffness happens from a lower value to a higher value, that is, during gap closure. Also, the intensity of these spikes was found to be more sensitive to the initial contact stiffness and the lateral velocity at impact rather than the amount of hysteretic ED. The VASs, caused by an impact of wall base with the foundation, also appear for a short interval of time and are also found to be dependent on the contact stiffness and the lateral velocity at impact, further signifying the importance of contact stiffness in the accurate modeling of dynamic behavior of rocking wall structures. Although there are some works regarding the quantification of vertical accelerations and its effects on the seismic performance of rocking bridge piers (Pollino and Bruneau, 2007), there is a lack of the literature focused on the VASs in rocking wall structures. The significantly higher values of HAS and VAS, found in the recent shake table tests (Belleri et al., 2014; Marriott, 2009; Toranzo, 2002), can result in an unintended shear slip failure at the wall base as a result of a concurrent increase in shear demand due to HAS and a decrease in shear slip capacity due to VAS. However, no work has been done to date to numerically model these acceleration spikes in rocking wall structures. Therefore, there is a need of numerical models that can predict these effects and hence can also be used for devising effective mitigation techniques to reduce these effects.

In order to successfully model the acceleration spikes produced as a consequence of the impact phenomenon, the contact behavior at the wall base needs to be modeled accurately. Two of the important parameters of the contact behavior are contact stiffness and contact damping. The initial contact stiffness of rocking wall before the gap opening has not been discussed enough in the literature, and usually, the rocking joint is assumed to be rigid initially. This assumption, although may not change the results much for a quasi-static analysis, can increase the intensity of acceleration spikes in a dynamic response

significantly and hence needs to be modeled carefully. Wiebe and Christopoulos (2009) modeled rocking wall contact behavior using a rotational spring at the wall–foundation joint with a flag-shaped hysteresis behavior. The numerically calculated horizontal acceleration values for top floor were found to be up to 17 g. However, this value is exaggerated because of the use of only one rotational spring with sharp-edged flag-shaped hysteresis and a relatively higher initial contact stiffness. On the other hand, Kurama (2002) modeled the rocking wall–foundation connection using a number of compression-only nonlinear springs at the base of rocking wall, resulting in a flag-shaped hysteresis behavior with rounded corners. He found that if sufficient amount of ED was provided to rocking walls, the peak roof lateral accelerations would be similar to the lateral accelerations in conventional RC shear walls.

The contact and impact phenomenon are also found to induce extra damping in the system response called as contact damping, primarily divided into two parts for an elastic contact: damping due to friction between the interacting surfaces (friction component) and due to stress wave propagation and other dynamic processes (viscous component) (Marriott, 2009; O’Hagan et al., 2013). Marriott (2009) found that both components are almost equal and represent a half of the contact damping. Recent experimental and analytical works (Marriott, 2009; O’Hagan et al., 2013) on rocking wall dynamic performance have suggested that the contact damping may have a negligible effect on the overall dynamic responses provided that a dedicated hysteretic ED mechanism is provided. However, in the absence of an external ED mechanism, this contact damping can dictate the dynamic response of two contacting bodies.

This study is focused on the investigation of impact-related acceleration spikes in rocking wall structures which includes the development of numerical models to predict these effects, identification of their effects on the overall dynamic performance, and the influence of different parameters on the severity of these effects which can also serve as a guideline for designing the effective solutions to reduce these acceleration spikes.

## Mechanics of rocking wall and contact

Generally speaking, modeling of structural pounding or impact can be classified into two types: the classical stereo-mechanical approach and the contact force model. The stereo-mechanical approach (Housner, 1963) assumes a contact of two rigid bodies with no sliding or bouncing and the response is controlled by the ED during contact called as contact damping. The parameter used to represent this change in the system energy is called as coefficient of restitution (COR). In a

rotational motion, the change in kinetic energy before and after impact due to contact damping can be quantified as

$$\frac{(\frac{1}{2}I_o\dot{\theta}_2^2)}{(\frac{1}{2}I_o\dot{\theta}_1^2)} = e^2 \quad (1)$$

where  $\dot{\theta}_1$  and  $\dot{\theta}_2$  are the rotational velocities before and after impact, respectively, and “e” is the COR. A COR value of 1 represents a fully elastic collision while a 0 value represents a fully plastic collision. The Housner model has been found to be accurate for the rigid blocks with a high slenderness ratio. However, the COR value alone cannot define the rocking response especially in the cases when the slenderness ratio is low, the block is flexible, or there is local damage at the contacting interfaces.

The contact force model is an alternative and a more sophisticated approach and takes into account the elastic and plastic behaviors of contacting bodies along with the damping or ED. Different contact force models present in the literature, with different combinations of linear and nonlinear stiffness and ED, are based on a general equation of contact force (Muthukumar and DesRoches, 2006)

$$F_c = F_E(\delta) + F_V(\delta, \dot{\delta}) + F_P(\delta, \dot{\delta}) \quad (2)$$

where  $F_E$ ,  $F_V$ , and  $F_P$  are the elastic, viscous, and plastic components of the contact force ( $F_c$ ), respectively, while  $\delta$  and  $\dot{\delta}$  are the relative penetration and penetration velocity during contact, respectively. The material properties, geometric properties, masses, and relative velocities of the interacting bodies are the different parameters that can influence the contact force behavior.

Elastic component of the contact force equation is dependent on the contact stiffness of contacting bodies and is usually characterized by the interaction of individual axial stiffness of each contacting body. For a rectangular rocking wall, contact stiffness can be idealized in the form of two axial springs acting in the series and representing the individual axial stiffness of rocking wall and foundation.

The viscous component of the contact force equation is usually modeled using Housner COR value. Different tests have been performed in the past to compare the experimentally calculated COR values with the Housner value for rectangular rocking objects. Nasi (2011) tested free rocking rectangular concrete blocks on shake table and the value of COR for any particular block was found to be changing with the varying initial conditions as opposed to a single COR value, for a particular rocking block, proposed by Housner. Ma (2010) described experimental and

numerical investigation of both free rocking (without PT steel) and controlled rocking (with PT steel) precast confined masonry walls. Experimentally calculated COR values were found to be close to the Housner value for the starting few cycles of free vibration response and then started to exhibit a low COR value (high ED) for lower initial conditions of initial displacement and the speed of impact. The COR values varied in the range of 0.5–0.95 with the varying initial conditions and he concluded that a single COR value cannot emulate the complete free vibration response. O'Hagan et al. (2013) separated the contact damping into two components: friction and viscous component. A constant friction force along with a COR value representing the damping due to dynamic effects found to give matching results for the entire range of the free vibration response. Cheng (2007) calculated the radiation damping of rocking bridge piers with different sizes of anchoring bars and contact surface materials along with the effects of sliding on the damping. Marriott (2009) tested four rocking walls: one without any external ED mechanism and three with different ED options. He quantified the contact damping in the first wall to be proportional to the secant stiffness and in the range of 1.8%–3% of equivalent viscous damping (EVD). Also, it was found that the contact damping was negligible for the walls with external ED mechanisms and it can be ignored in the modeling of dynamic behavior of hybrid walls. The plastic component of the contact force equation is assumed to be absent in the rocking wall structures due to the damage avoidance design of these members. In this study, contact force approach is used to model the dynamic behavior of a case study rocking wall.

### Case study building

There are only few works in the past where the shake table testing of a rocking wall structure is carried out and the acceleration spikes in both lateral and vertical directions are measured. Most of these tests were conducted on single rocking walls. Dynamic models of single rocking walls rely heavily on the use of a proper contact damping model to accurately predict their dynamic behavior. However, in a realistic and complete rocking wall structural system, the contact damping may become negligible when compared with the other sources of damping. The shake table test conducted by Schoettler et al. (2009) on a three-story, half-scale rocking wall structure is one test where a complete rocking structural system was tested, and the acceleration spikes in rocking walls were measured using accelerometers. Also, detailed results of all the dynamic tests performed by Schoettler et al. (2009) are publicly available (web address in references; Data

repository, n.d.), making it a suitable choice for numerical model verification in this study. The case study structure was tested as part of a Diaphragm Seismic Design Methodology (DSDM) project on Network for Earthquake Engineering Simulation (NEES) outdoor shake table located at the University of California San Diego as shown in Figure 2(a). The building structure was designed with two rocking walls, providing the primary lateral force resistance on both the north and south ends. The gravity load-resisting system consists of three different precast flooring types on three floors, five precast columns on each side, and spandrel and ledger beams to support the flooring on the two sides. It is important to note that the gravity load-resisting system was designed to be flexible so as to contribute least to the lateral shear demand. Also, a special vertical slotted connection was designed for wall-to-floor connection which prevented the vertical actions from the wall to be transferred to the flooring units.

A number of earthquake excitations were provided to the structure in east (E)–west (W) direction. For the first low-intensity Knoxville design basis earthquake (DBE) test, no ED mechanism was used for rocking wall and an initial PT of 472 kN ( $0.26f_{pu}$ ) was provided through two ducts each containing five 0.5-in diameter low-relaxation unbonded PT strands (Grade 270). For higher intensity tests, two ED bars were grouted in the wall–foundation joint. Initial PT force was increased to 642 kN ( $0.35f_{pu}$ ) for each wall to counter the higher demand. PT and ED steel were provided at an offset of 300 and 150 mm from the center on each side, respectively. Rocking walls were specially designed in the wall toes to resist the extreme compression forces due to gap opening and extra confinement reinforcement was provided in the toe regions. Also, steel plates were used in the wall corners which further increased the confinement and also kept the damage in the toe region to a minimal value. Further information about the design procedure, construction, instrumentation, and experimental results can be found in Belleri et al. (2014), Schoettler (2010), and Schoettler et al. (2009).

For this study, the numerical results are compared with the experimental results of first two tests, namely, Knoxville DBE and Seattle DBE representing low and moderate seismic hazards, respectively. Response spectrum of excitation histories is shown in Figure 2(c). Since the case study building was designed as a symmetrical structure with two walls at north and south ends responsible for providing primary lateral force resistance to the structural system against seismic actions in E–W direction, only half of the structure can be modeled to study the dynamic behavior of overall structure. On the other hand, gravity columns were found to be contributing 12% and 9% to the system overturning moment resistance and 24% and 21% to the system

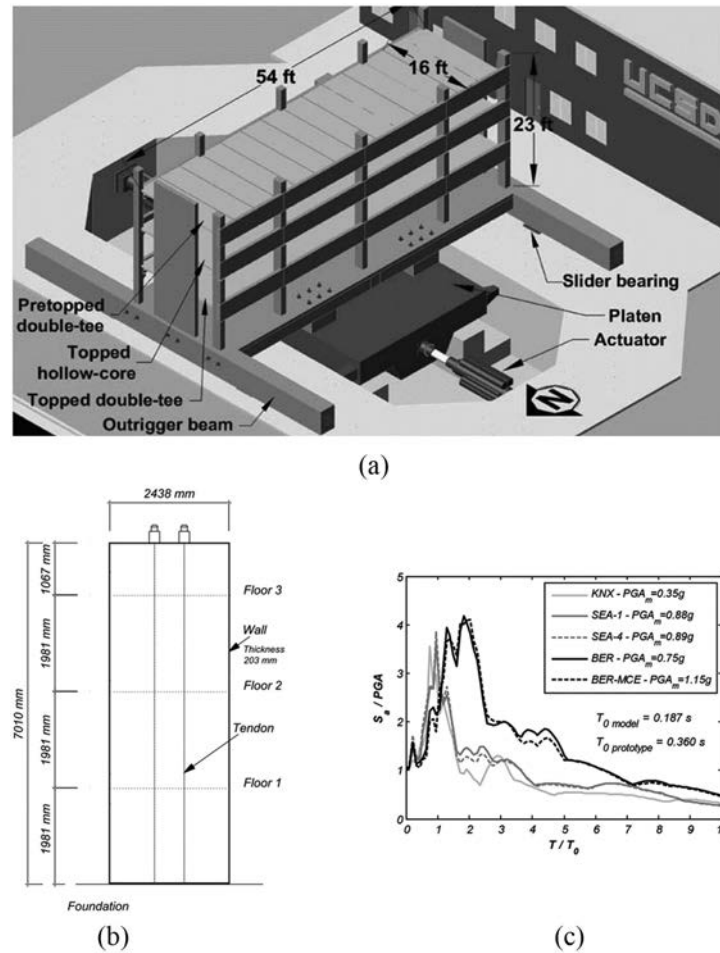


**Figure 2.** (a) 3D view of case study building (Schoettler et al., 2009), (b) dimensions of rocking wall, and (c) response spectrum of excitation histories (Belleri et al., 2014).

shear resistance at peak response for the Knoxville DBE and Seattle DBE tests, respectively (Belleri et al., 2014). So one of the rocking walls is modeled in this study as a representative of half of the symmetrical structure. Figure 2(b) and Table 1 show the dimensions and important parameters of the rocking wall considered here.

**Contact modeling of rocking wall**

Now for the modeling of the case study rocking wall, different components of the contact force equation are selected. A lot of work done in the past on the dynamic modeling of contact behavior is based on the stereo-mechanical approach. This approach assumes that there is no sliding or bouncing between the contact of the rigid block and its rigid base, and that the ED can be modeled using the COR. Although more recent studies have incorporated the flexibility of rocking blocks and the possibility of sliding or bouncing phenomenon in the numerical models, most of this work

was focused on free rocking blocks. A rocking wall, however, is different from a free standing block due to the presence of PT tendons. Its controlled rocking mechanism creates new challenges for modeling. As explained earlier, past works on the modeling of rocking walls were focused on the development of more elaborate contact damping models using mathematical approaches (Ma, 2010; O’Hagan et al., 2013) and simplified multi-spring or fiber models (Marriott, 2009) to predict the displacement response and ED of single rocking walls; however, the ability of these models to predict acceleration spikes has never been checked so far. Finite element (FE) models using implicit techniques have also been used in the past for both free rocking and controlled rocking systems. Belleri et al. (2013) conducted dynamic analysis of a rocking wall using different modeling techniques including a three-dimensional (3D) FE model, one-dimensional (1D) fiber model, and multi-spring model with a relatively rigid contact for all models. The effect of different damping models on the dynamic responses of rocking

**Table 1.** Properties of case study rocking wall.

Thickness of wall (mm)		200
Compressive strength of wall concrete ( $f'_c$ ) (MPa)		51
Ultimate strength of PT steel (MPa)		1860
$P_u/(f'_c A_g)$ (%) <sup>a</sup>	Knoxville DBE	2.7
	Seattle DBE	3.5
Total lateral seismic masses (kg)	First floor	36,795
	Second floor	38,999
	Third floor	34,230
Vertical seismic mass (kg)		8064

PT: post-tensioning; DBE: design basis earthquake.

<sup>a</sup> $P_u$  is the axial load;  $A_g$  is the gross area of wall.

wall was studied; however, the proposed models were not validated against the experimental results.

As opposed to the previous works on rocking walls where a relatively rigid contact was used, the FE model in this study adopts the actual material properties of rocking wall and its foundation, resulting in a realistic and flexible contact behavior. As the case study rocking wall was designed on the principle of damage avoidance design and the damage during the experimental tests was found to be restricted to the grout crushing with only minor cracking in the rocking members (Belleri et al., 2014), a linear-elastic material model is used for the rocking wall and the foundation. The value of contact stiffness is an important issue as it can have a significant effect on the severity of acceleration spikes. Contact stiffness value depends on the individual behavior of interacting bodies and it has been found to vary with the varying level of gap opening.

Inherent damping of rocking wall structures including the contact damping is usually less than the conventional structures because of the limited damage in the rocking members. Different tests and numerical studies performed in the past on a number of rocking wall structures have shown that a consistent modal damping of 3% is suitable for the modeling of inherent damping of these structures (Priestley et al., 1999; Toranzo, 2002). Also, Belleri et al. (2013) proposed a consistent 3% damping for all modes of excitation for the same case study building as in this study. In contrast to the earlier works on single rocking walls, the inherent damping of the case study building represents the damping due to the microscopic and macroscopic processes within the flooring units, beams, columns, and rocking walls along with the friction damping at the beam–column, flooring–wall, column–foundation, and wall–foundation joints as well as the contact damping. This means that the contact damping may become negligible when compared with the other

sources of damping. Therefore, a simple damping model, that is, 3% inherent damping for all the modes without explicitly modeling the contact damping, is assumed to be suitable for this study. Finally, as the damage incurred to the wall during dynamic testing was reported to be minimal, plastic component of the contact force equation is ignored. Seismic masses in horizontal direction represent the floor masses along with the contributions from beams and columns mass and are shown in Table 1.

In the first part of this study, a 3D FE model of the case study rocking wall is created in ABAQUS 6.12 (ABAQUS, 2012) to model the gap opening and horizontal acceleration responses. The sophisticated contact algorithms available in ABAQUS platform are particularly useful in calculating and using appropriate contact stiffness values for each contact and hence can be helpful in drawing a general assumption for contact stiffness value to be used for a simple and computationally inexpensive multi-spring fiber model. This simple computer model will then be used for the modeling of both horizontal and vertical acceleration responses.

## FE model of rocking wall

3D solid FE model of the case study rocking wall is shown in Figure 3. The proposed model makes use of an explicit FE analysis—a suitable approach for modeling high-speed contact problems. Different advantages of using explicit FE analysis include a relatively inexpensive and fast procedure, ability to accommodate the material and geometric nonlinearities, and the absence of a convergence criteria requirement as opposed to implicit analysis. The rocking wall and foundation are modeled using the element-type C3D8R—eight-node linear brick elements with reduced integration to reduce the solution time. Hourglass control is also used to control the effects of hourglass modes due to the use of reduced integration elements. As decided in the previous section, a linear-elastic concrete material model is used for the wall and the foundation. The modeling of the grout at the wall–foundation joint is ignored by following the guidelines proposed by Smith and Kurama (2012). The gap opening behavior at wall–foundation joint is modeled using a contact interaction with a “hard contact” which means no plastic indentation under compressive stresses while allowing unrestricted gap opening. Also, a no-slip condition is defined to prevent any shear slip which is in accordance with the experimental testing where shear keys were provided at the wall toes to avoid any slip. A mesh size of  $50 \times 50 \times 50 \text{ mm}^3$  is used for the wall while for the foundation mesh size is

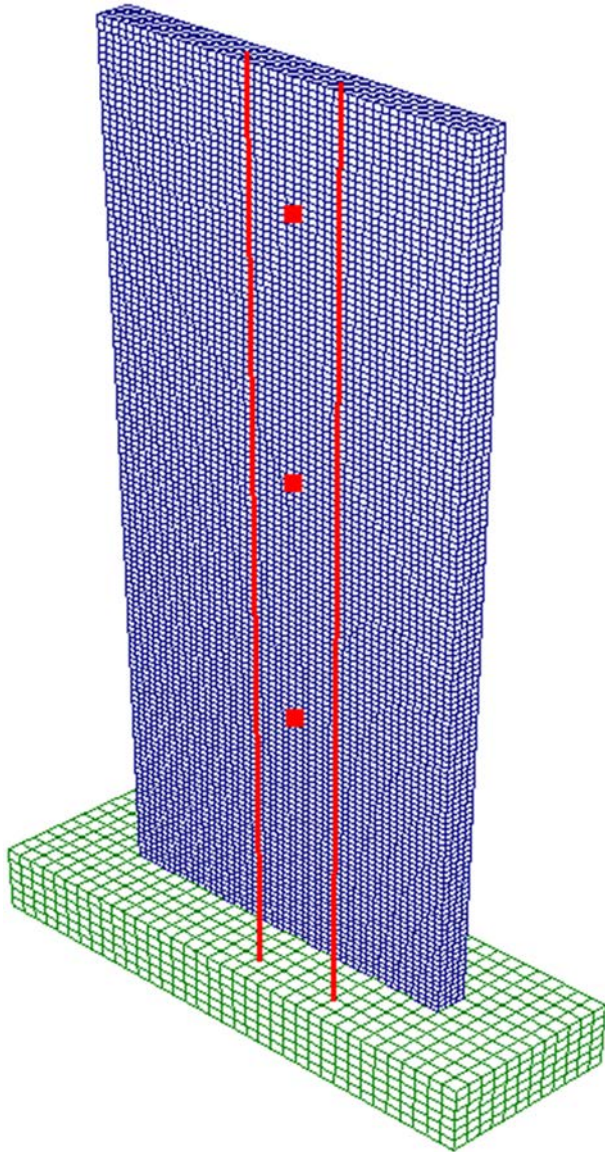


**Figure 3.** 3D finite element model.

selected as  $100 \times 100 \times 100 \text{ mm}^3$ . A mesh sensitivity study is done before selecting these particular mesh sizes. PT steel is modeled using two-node 3D truss members (T3D2) with nonlinear stress-strain properties found from the material testing. The horizontal and vertical degrees of freedom of the top tendon node are coupled with a corresponding node on the rocking wall to model the anchorage at the top. This constrained the displacement of the top tendon anchorage to the displacement of the wall panel. The bottom tendon anchorage is represented by restraining the horizontal and vertical degrees of freedom of the bottom tendon node (pinned connection). No interaction is defined in the middle portion of the PT steel with the wall to model the unbonded property of PT steel.

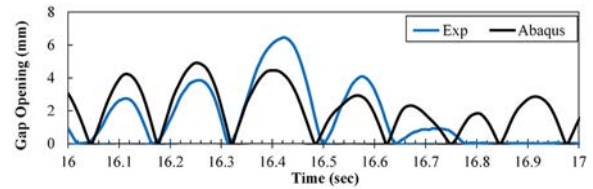


**Figure 4.** Gap opening for Knoxville test.

### FE model results

It should be noted here that the case study structure was proportioned as a symmetrical structure with two rocking walls on the north and south corners. The rocking walls were designed with a duct for PT steel in the center while two ducts were provided for ED bars at an offset from the center on both sides. The ED ducts were designed to be un-grouted for the first Knoxville DBE test (no ED) and grouted for the remaining tests. However, one of the ducts for ED bars in the south wall was accidentally partially grouted in the first test which increased the lateral stiffness of the south wall. This resulted in a relatively lower gap opening in south wall and a relatively higher gap opening in the north wall but still showed an almost similar pattern of gap opening and closing in both walls. Past works have shown that the intensity of HASs in a rocking wall can be affected by the level of hysteretic ED capacity of that particular wall (Toranzo, 2002). Since the level of ED provided by the one partially grouted duct in south wall cannot be accurately emulated, it is considered reasonable to model the rocking wall without any ED mechanism and compare the numerical model results with the north wall experimental results. Figure 4 shows the comparison of the experimental and numerical results for the gap opening of the north wall. Pattern of gap opening and closing is quite similar for the numerical and experimental results; however, the numerical model results show a significant underestimation of peak gap opening values which is expected due to the reasons explained above. Figure 5 shows the comparison of base moment-rotation relationship for the numerical model results with the experimental results of both the south and the north walls. Albeit some underestimation, the numerical model moment-rotation results are relatively more comparable to the north wall experimental results, as assumed in the above discussion.

The amplitude of accelerations recorded in a structure is quite sensitive to the time step being used or the highest frequency that can be captured with the available instrumentation. For this case study building, experimental data were recorded at a time step of 4.2 ms and was later on filtered using a low-pass filter with a cutoff frequency of 33 Hz. So for the numerical

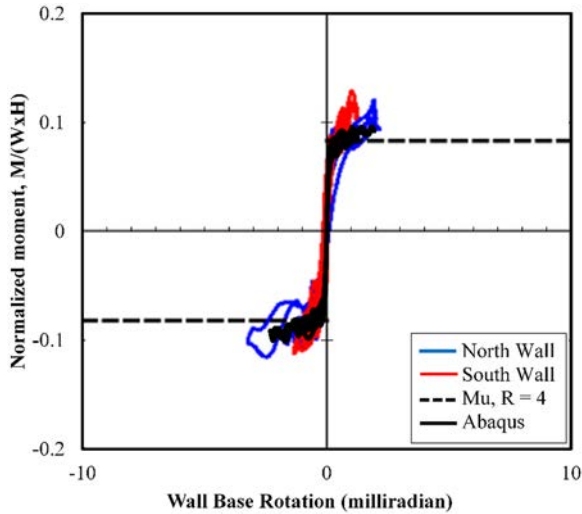


**Figure 5.** Moment–rotation relationship for Knoxville test.

model results, similar time period is used in the dynamic analysis and then the results are filtered with a cutoff frequency of 33 Hz. Figure 6 shows the comparison of horizontal acceleration ( $a_h$ ) values at the top floor for the experimental and numerical results. The numerical horizontal acceleration values predicted by ABAQUS generally match well with the experimental results except a slight underestimation. This may be due to the reduced gap opening observed in the numerical results. Horizontal accelerations considered with the gap opening show that there are two kinds of peaks in the response history. One is linked to the maximum displacement time instant while the other

one appears during the opening and closing of the gap. Latter one is a unique characteristic of rocking and base isolation structures. It is important to note that the horizontal acceleration peaks associated with the impact are higher than the peaks against the maximum drift. This much high acceleration against the minimal base rotation demands a new limit state to be identified in the design procedure and the shear slip capacity needs to be checked against this new limit state.

The comparison of the results shows the effectiveness of FE model in emulating the contact stiffness behavior and predicting the dynamic responses with significant accuracy, and hence, it can be used to predict the contact stiffness value. Looking at the axial stress variations in the rocking wall against different levels of gap opening reveals that the variation in the height of the wall contributing to the axial stiffness of rocking wall, found from the FE model, is in the range of  $0.1\text{--}1.0L_w$  for the different levels of lateral drift. Although the FE model is found to be quite efficient in predicting the dynamic responses of case study rocking wall, it is computationally more expensive. So a more robust and computationally economical multi-spring fiber model is used.

### Multi-spring fiber model

Multi-spring fiber model is created in a commercially available software Ruaumoko 2D (Carr, 2004) as shown in Figure 7. Wiebe and Christopoulos (2010) described that HAS is a manifestation of the abrupt stiffness change in a bilinear elastic or flag-shaped

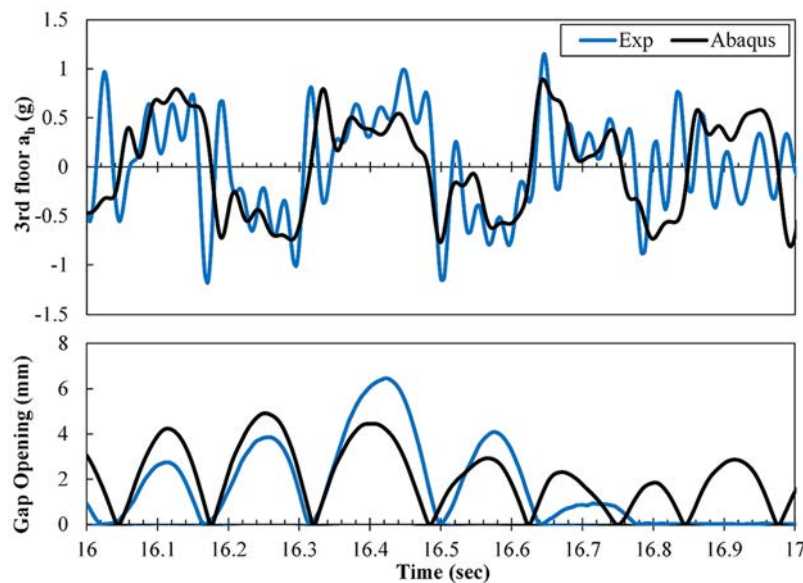


**Figure 6.** Lateral roof acceleration for Knoxville test.

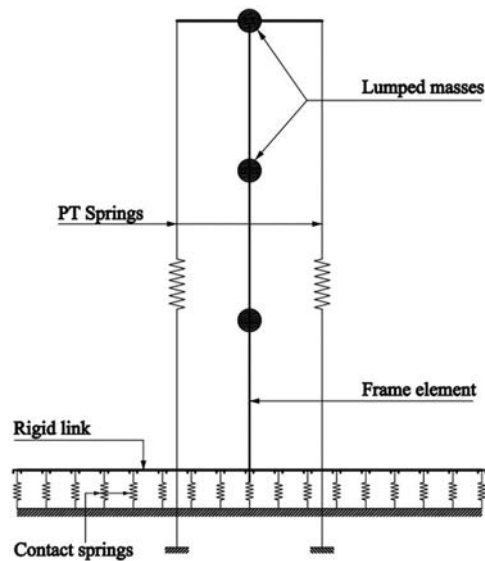


Figure 7. Multi-spring fiber model.

hysteresis and although it is a physical phenomenon, yet the choice of modeling options can amplify this. For example, use of a rotational spring at the wall base with a sharp-edged flag-shaped hysteresis would increase HAS unjustifiably. So a better way of modeling is to model concrete, PT steel, and ED mechanism separately along with the use of a number of axial springs to model the contact phenomenon, resulting in a realistic flag-shaped hysteresis behavior with relatively smooth corners. This latter approach has been adopted for the multi-spring fiber model. Rocking wall is represented by an elastic frame element as the wall is expected to remain elastic against seismic actions. PT is modeled using nonlinear springs with elasto-plastic behavior. Initial PT is provided using pre-load option available in Ruaumoko 2D. Nonlinear behavior of gap opening is modeled using a number of compression-only contact springs which are fixed at the base and are connected to a rigid member at the top to simulate plane section remain plane behavior. Spieth et al. (2004) suggested in his study that at least 8 base springs should be used to efficiently predict the neutral axis migration for the modeling of a rocking beam while Pennucci (2008) used 20 springs for the modeling of rocking wall. In this study, 25 base springs have been used due to a longer cross section of the wall. Contact stiffness of the base springs is the interacting stiffness of the wall and the foundation, and can be modeled using two springs in series representing the axial stiffness of the wall and foundation. Assuming that the foundation is near rigid, rocking wall axial stiffness can be used as contact stiffness. Axial stiffness of the rocking wall can be calculated using the relationship

$EA/H_w$ , where  $E$  is the elastic modulus of concrete,  $A$  is the influence area of the spring, and  $H_w$  is the height of the wall that is providing the axial stiffness. Multi-spring fiber model requires a constant value of contact stiffness for any particular contact spring. Conley et al. (2002) calculated contact stiffness of a rocking wall, tested as a part of precast seismic structural system (PRESS) program, by assuming a concrete deflection of 0.5 mm for a force of 890 kN which would yield a contact stiffness value of 1780 N/mm  $\approx EA/0.5L_w$ , where  $L_w$  is the wall length. Marriott (2009) proposed an empirical equation for an approximate estimate of contact stiffness which yields a contact stiffness value equal to  $EA/0.45L_w$  for this case study rocking wall. Belleri et al. (2013) modeled the same case study building as in this study and used a contact stiffness of  $EA/0.15L_w$  assuming that the wall height equal to the neutral axis depth against the maximum rotation represents the axial stiffness of rocking wall. However, this value was found to be overestimating the acceleration responses. Spieth et al. (2004) suggested a contact stiffness of  $EA/0.5L_w$  for the modeling of rocking beam-column connection and concluded that the results were not sensitive to the contact stiffness value. Although this may be true for quasi-static response, dynamic response of rocking walls especially the acceleration spikes could be sensitive to the contact stiffness value.

As described above, a number of different contact stiffness values have been used in the past ranging from near-rigid stiffness to the empirically deduced values from the experimental results with no agreement on a particular value and without the realization of its effects on the dynamic responses. Based on the findings from the FE model where the significant axial stresses in the rocking wall were varying from  $0.1L_w$  to  $1L_w$ , three different contact stiffness values of  $0.5K_b$ ,  $1K_b$ , and  $3K_b$  representing wall heights equal to  $1L_w$ ,  $0.5L_w$ , and  $0.16L_w$ , respectively, are used, where  $1K_b$  is equal to  $EA/0.5L_w$ . Inherent damping and lateral lumped masses are the same as described earlier for the FE model.

### Multi-spring fiber model results

Figure 8 shows the results for gap opening and horizontal accelerations ( $a_h$ ) using different contact stiffness values. The HAS results with contact stiffness of  $1K_b$  and  $3K_b$  are quite similar and matches with the FE model results with almost similar level of accuracy. A lower stiffness value ( $0.5K_b$ ) is found to reduce the overall response while a higher stiffness value ( $3K_b$ ) tends to increase the response quantities. The change in contact stiffness value is also found to change the gap opening values both in magnitude and in phase. The effect of different contact stiffness values will be further

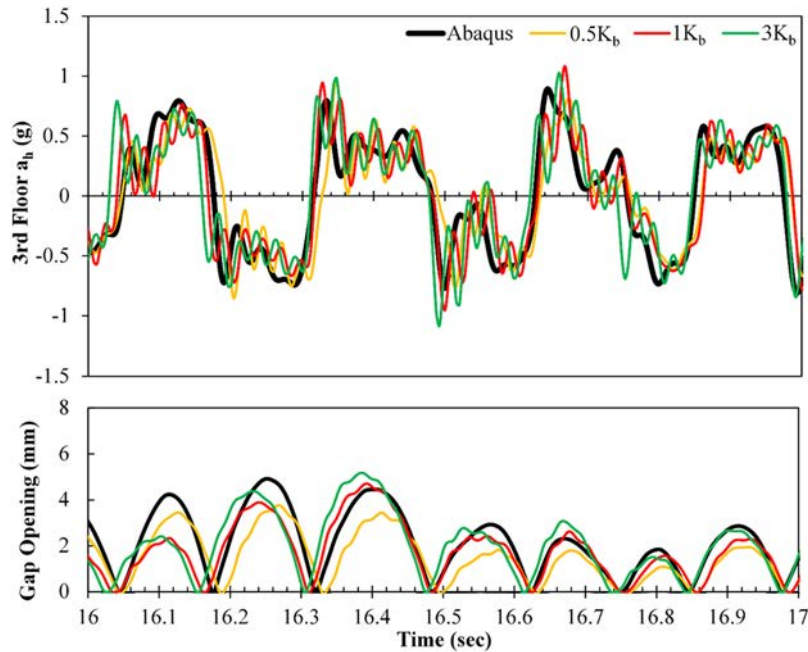


**Figure 8.** Effect of contact stiffness variation on HAS.

**Table 2.** Axial modal properties of rocking wall.

Mode No.	Period (s)	Mass participation (%)
1	0.0073 (137 Hz)	92.8
2	0.0026 (384 Hz)	6.6
3	0.0018 (555 Hz)	0.5

checked for the VAS results also before suggesting a particular value of contact stiffness as a better approximation of the actual varying contact stiffness value.

Now for the second part, modeling of vertical accelerations will be tried. Different seismic codes and nuclear regulatory guides have explained the concept of rigid frequency defined as the minimum frequency after which the curves for various damping ratios have similar values of spectral acceleration. A usual value of this rigid frequency is 33 Hz and the response of modes whose natural frequency is greater or equal to this frequency is considered to be quasi-static rather than dynamic. The spectral acceleration for such modes becomes equal to the PGA and is usually referred as zero-period acceleration. The natural frequencies of the case study rocking wall in vertical direction are well beyond this limit of 33 Hz as shown in Table 2 implying that the vertical acceleration response is in rigid range. This is also validated by the experimental results where the vertical accelerations at different story levels are almost identical and the vertical response is quasi-static. Nevertheless, the vertical accelerations if transferred to the floor could harm the flooring units and

the nonstructural elements such as fire suppression systems, emergency power generators, and computer systems attached to the floors. In this case study building, floors were separated from the walls and hence, vertical accelerations were not transferred to the flooring. Still, it is worth checking during the design of rocking wall structures that whether the vertical accelerations should be allowed to transfer to the flooring or not and thus design the flooring units and the floor-wall connections accordingly.

Contact damping is an important parameter for the modeling of vertical response as it decides the lateral velocity at impact and also acts in the dissipation of vertical responses. As explained earlier, the previous works on the modeling of contact damping have separated the contact damping into two parts and are modeled separately. These components were applied to the lateral displacement and lateral velocity to mimic the friction and viscous components. In reality, a part of contact damping comes from the loss of kinetic energy in the vertical direction. However, this vertical component of contact damping in rocking wall structures has not been focused in any experimental or theoretical work, and therefore, no guidelines are available to separate this component to provide damping to the vertical mode of excitation. Marriott (2009) described that the vertical accelerations are directly proportional to the lateral velocity at impact regardless of the amount of contact damping. He further concluded that two walls with different damping contents can experience similar peak vertical accelerations during rocking if

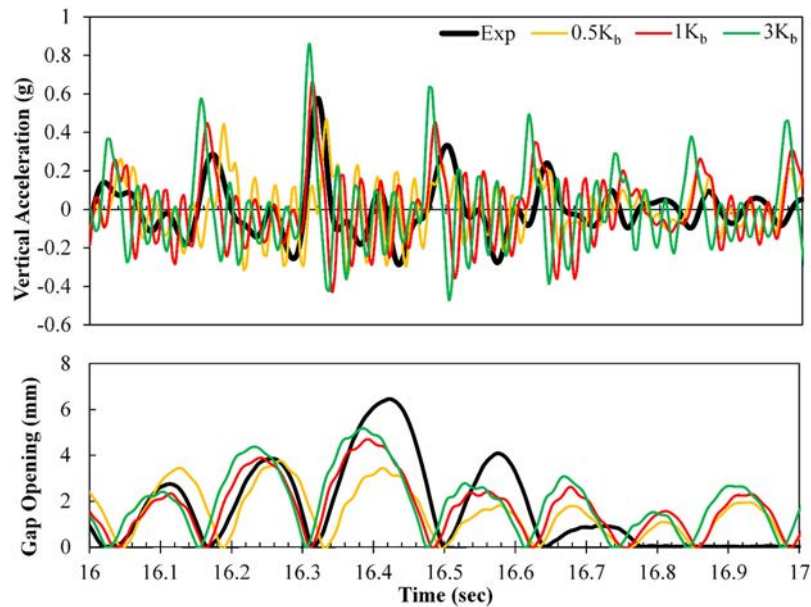


**Figure 9.** Effect of contact stiffness variation on VAS.

both are subjected to similar peak horizontal velocity demands. Hence, the accurate modeling of vertical acceleration response needs an accurate lateral velocity at impact along with a reasonably accurate value of contact stiffness while the vertical component of contact damping would only be required to dissipate the vertical response. Similar observations were made by Wiebe and Christopoulos (2010) about the dependency of lateral accelerations on the lateral velocity and contact stiffness with no effect coming from the damping. Now, since the fiber model is found to be predicting the lateral acceleration and lateral velocity with reasonable accuracy, the vertical acceleration response can be modeled by giving the seismic masses in vertical direction and by ignoring the explicit modeling of vertical component of contact damping. The vertical seismic masses here represent the rocking wall seismic mass only due to the presence of sleeved connection.

Figure 9 shows the results for gap opening and vertical accelerations using different contact stiffness values. The results show that the use of a higher contact stiffness value ( $3K_b$ ) increases the VAS significantly while a lower contact stiffness decreases the VAS values and also changes the gap opening both in magnitude and in phase. Looking at the results of HAS and VAS against the different contact stiffness values, the results with  $1K_b$  seem to be matching better with the experimental results compared with the other two options. The approximation of using a constant contact stiffness value for each particular spring proves to be a valid assumption and can be used in the future works provided that a reasonable value is chosen in

the first place. Figure 10 shows the comparison of the experimental and numerical results for both lateral and vertical accelerations along with the gap opening calculated using a contact stiffness of  $1K_b$ . It is clear from the results that the inclusion of the vertical seismic masses does not affect the lateral responses much. It is quite evident by considering vertical acceleration history together with the gap opening history that vertical acceleration peaks are directly related to the impact of wall base with the foundation. The comparison of vertical acceleration shows a significant matching of peak values and a relatively slower dissipation of vertical response in the numerical results as compared to the experimental results which is expected. The matching of the peak values without providing any contact damping in the vertical direction validates that the vertical accelerations are more sensitive to the lateral velocity and the contact stiffness rather than the contact damping and a realistic estimate of vertical acceleration envelope values can be obtained without explicitly modeling the contact damping in vertical direction.

Figure 10 further shows that both these accelerations develop peaks at approximately the same time and could be a cause for a shear slip failure along the wall–foundation joint. This has been mentioned in the previous works also (Belleri et al., 2014). Now considering a coefficient of friction of 0.5 for concrete–concrete contact, the changes in the shear slip capacity at the wall–foundation joint are calculated using vertical seismic mass and vertical acceleration. Figure 11 shows the time history of shear demand and shear slip

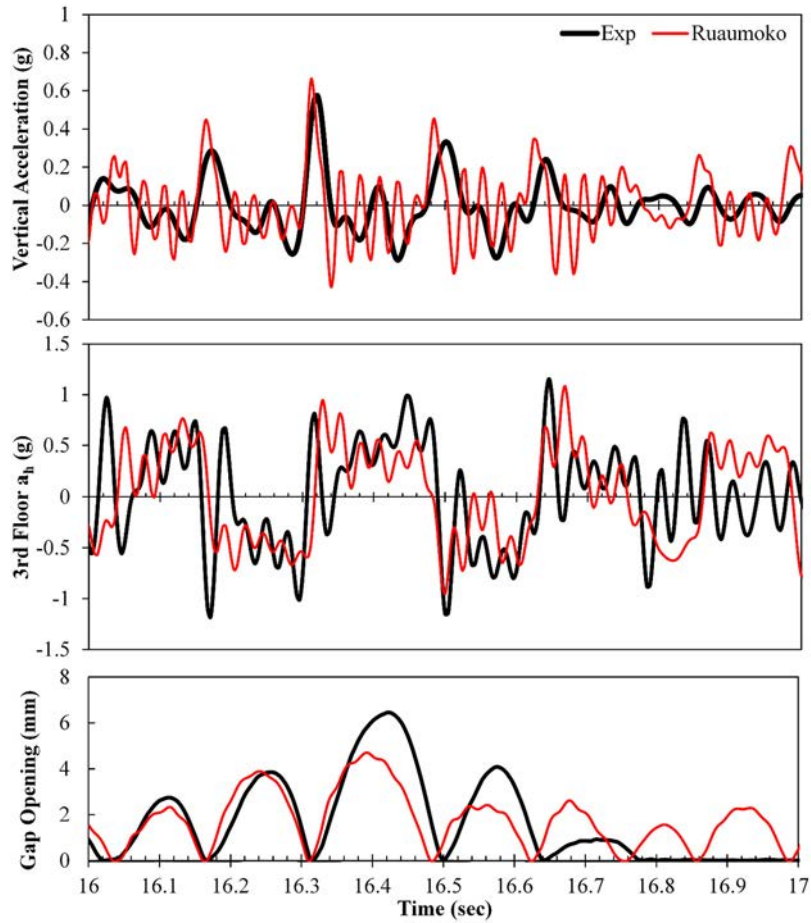


Figure 10. Comparison of acceleration spikes for Knoxville test.

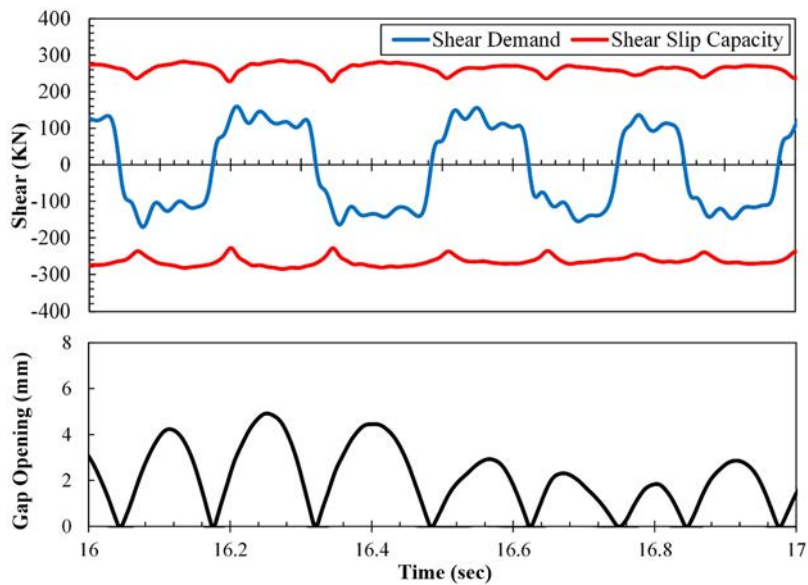
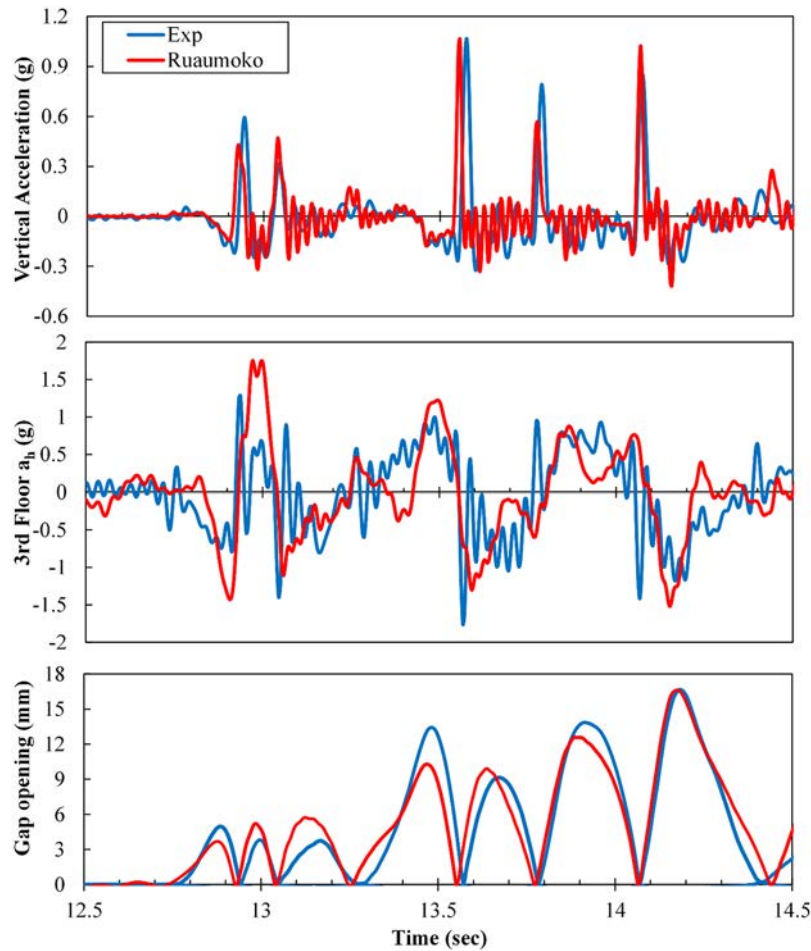


Figure 11. Effect of HAS and VAS on shear demand and shear slip capacity for Knoxville test.



**Figure 12.** Gap opening, HAS, and VAS for Seattle test.

capacity for the first test. The results show a 10% (25.8 kN) decrease in shear slip capacity during gap closure and also there is an increase in the shear force at the same time.

Based on the findings from the first test, Seattle DBE test is modeled by Ruaumoko 2D. In this test, two ED bars were used in the wall–foundation joint to provide ED in addition to the contact damping. The results of gap opening for Seattle DBE excitation match at a lower contact stiffness of  $0.4K_b$ . One of the reasons for a lower stiffness value is that a number of tests were performed on the same structure prior to Seattle DBE test. So the structure was softened due to grout crushing, nonstructural damage, and minor cracking in the rocking members and hence exhibited a lower stiffness value. Once the gap opening values match, numerical model is able to predict impact-related accelerations quite efficiently. Figure 12 shows the histories of HAS and VAS along with the gap opening history. Similar to the previous test, horizontal acceleration peaks against the impacts are higher as

compared to the peaks related to the maximum rotation while the VAS is directly related to the impact of the wall base with the foundation and its envelope values are predicted by the numerical model quite efficiently. Time history of shear demand and shear slip capacity, assuming a coefficient of friction of 0.5, is shown in Figure 13. The reduction in shear slip capacity during the gap closure is calculated to be 12% (42.5 kN).

### Control measures for acceleration spikes

Toranzo (2002) and Schoettler (2010) tested rocking and hybrid walls on shake table and concluded that the addition of ED mechanism causes a smooth and gradual change in stiffness during gap opening and closure, resulting in a decrease in the HASs. Also, a softer contact at wall base helps reducing the higher frequency content of lateral accelerations (Conley et al., 2002). However, VASs were found to be least sensitive to the absence or the presence of a dedicated external

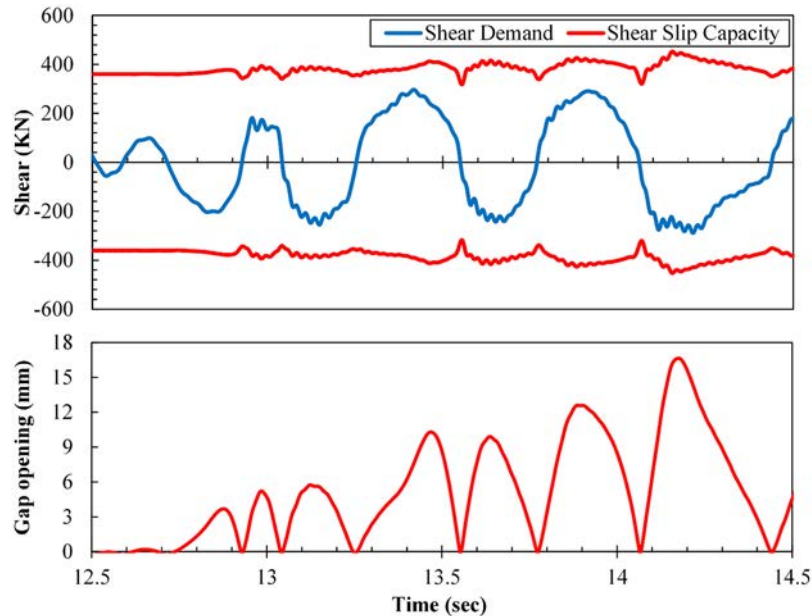


**Figure 13.** Effect of HAS and VAS on shear demand and shear slip capacity for Seattle test.

ED mechanism. To further understand the nature of impact-related vertical accelerations, a rocking wall is selected with dimensions of  $3000 \times 1000 \times 150 \text{ mm}^3$ . The single-story rocking wall is part of a complete structural system and is assumed to take all the lateral load of the structure. The connection between flooring unit and the rocking wall is assumed to be similar to the one being used for the case study structure discussed in this study. The lumped mass in the lateral direction represents the floor load while the vertical seismic mass is the mass of the rocking wall only. For simplicity, only one vertically lumped mass is used at the top of the wall. Design spectra for this study are assumed to be representing a high seismic hazard site. The rocking wall is designed against the desired moment capacity using three different configurations. The first type represents a rocking wall with only PT steel and no ED mechanism, and is referred as RW1. The second type represents a hybrid wall with a displacement-dependent ED device (mild-steel) placed at the wall-foundation connection. RW3 represents a rocking wall with PT steel and velocity-dependent energy dissipater such as viscous damper placed at the wall toes on both sides. For the hybrid walls (RW2 and RW3), PT steel and weight of the rocking wall are designed to take 55% of the lateral load with 45% being resisted by the ED mechanism to ensure the self-centering mechanism. Three different ground motions, matched with the design spectra, are selected for the nonlinear dynamic analysis of the rocking wall structures. Contact stiffness and inherent damping are selected

based on the findings from the modeling of dynamic test in this study. It is important to note here that we are not interested in the values of vertical accelerations rather the effects of different parameters on the vertical acceleration response will be discussed.

Figure 14 shows the unfiltered results of vertical accelerations for three rocking walls plotted against the lateral drift at wall top. As expected, the vertical accelerations appear in the response when the lateral drift is close to 0, that is, when the wall base impacts with the foundation. The lateral drift values for RW1 are highest followed by RW2 and RW3, respectively, for the same set of ground motions. The vertical acceleration response plotted against the lateral velocity, as shown in Figure 15, shows that the intensity of vertical accelerations is directly proportional to the lateral velocity of the wall. The relationship between the two seems to be linear and can be represented by a straight line joining all the peaks of the vertical acceleration values. The vertical acceleration values for RW2 seem to be high as compared to RW1 for the similar level of lateral velocity. On the other hand, RW3 seems to have a similar level of vertical acceleration intensity as compared to RW1 for any particular lateral velocity during impact. The comparison of RW2 and RW3 shows the effectiveness of velocity-dependent damper in reducing the VASs. RW3 not only has a lower level of vertical acceleration value for any particular lateral velocity during impact but also is quite useful in reducing the lateral velocity which, in turn, reduces the vertical acceleration value. The slope of the line joining all the

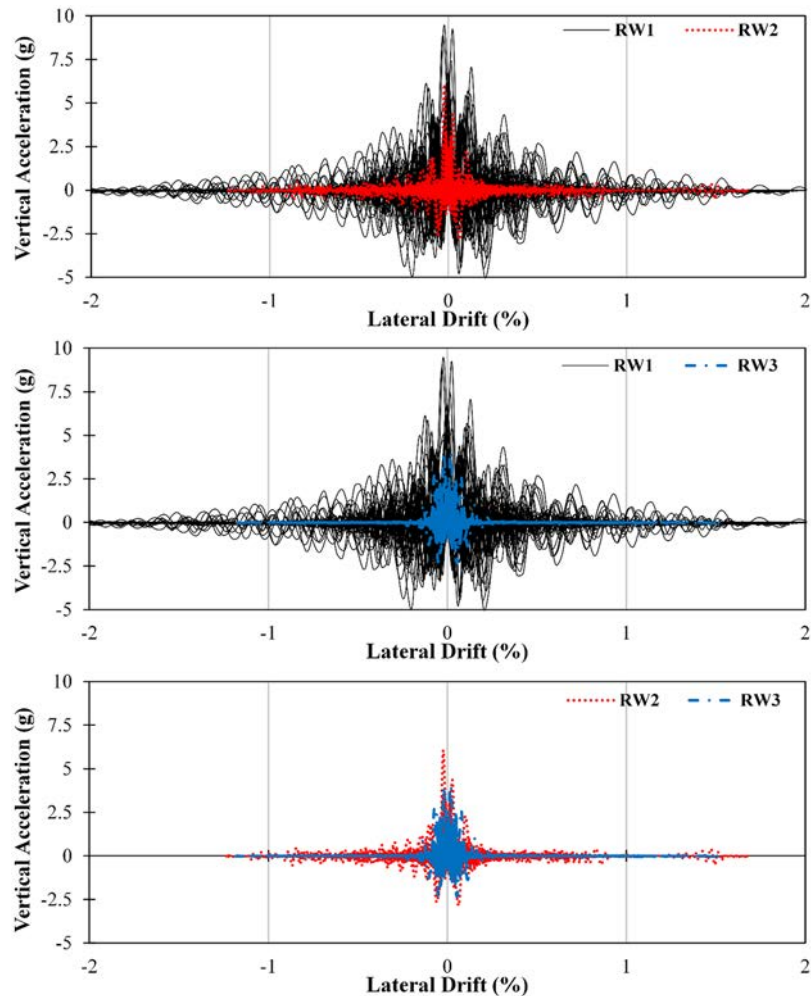


**Figure 14.** Vertical accelerations plotted against lateral drift.

peaks is found to reduce by reducing the contact stiffness between the rocking wall and the foundation. To reduce the VASs, a combination of a relatively softer contact and the presence of velocity-dependent damper on the wall corners would be an effective solution.

## Conclusion and recommendations

This study is focused on the development and validation of numerical models to predict the impact behavior and the dynamic responses associated with it for a controlled rocking system. As opposed to the previous works focused on the modeling of displacement behavior and the contact damping by considering the impacting bodies to be relatively rigid, the FE model developed in this study takes into account the flexibility of the contacting members and assumes a simple yet realistic damping model. Also, the FE model makes use of a more suitable FE explicit analysis and a

reduced integration technique to increase the efficiency and decrease the solution time, respectively. Albeit some underestimation, the proposed FE model is shown to predict the gap opening and the lateral acceleration spikes with reasonable accuracy. Furthermore, a simpler multi-spring model with spread plasticity at the wall base and with a constant contact stiffness value, proposed using a careful review of finite element and multi-spring model results, is found to predict both the lateral and vertical acceleration responses reasonably well. The results show that the intensity of horizontal acceleration peaks associated with the impact is higher than the peaks against the maximum drift for both tests considered in this study. The vertical acceleration response, on the other hand, is found to be in the rigid range. Still the high-frequency vertical accelerations, if transferred to the flooring units, can cause damage to the flooring and the nonstructural components. Therefore, a parametric study is done

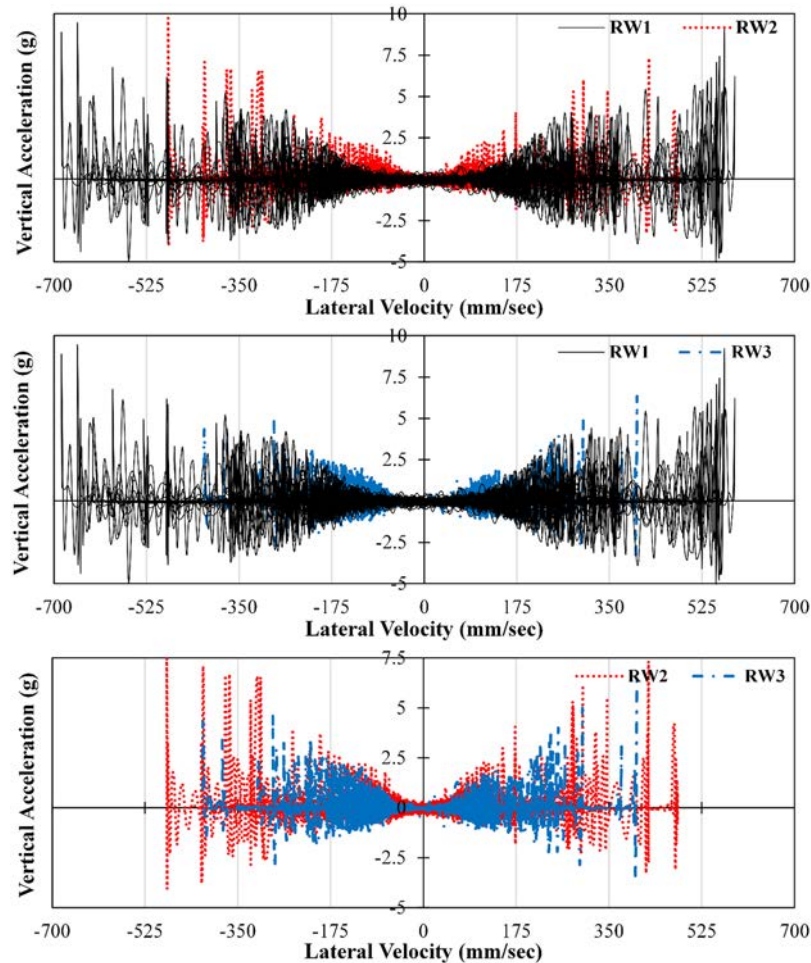


**Figure 15.** Vertical accelerations plotted against lateral velocity.

using different ED options in a rocking wall to understand their effect on the vertical acceleration response. The results show an almost linear relationship between the vertical acceleration and the lateral velocity at impact while the slope of this linear relationship is found to be highly dependent on the contact stiffness. Based on the results, it is proposed in this study that a combination of reduced contact stiffness and the use of a velocity-dependent damper is an effective solution for mitigating the high-frequency vertical accelerations in rocking walls.

#### Declaration of Conflicting Interests

The author(s) declared no potential conflicts of interest with respect to the research, authorship, and/or publication of this article.

#### Funding

The author(s) received no financial support for the research, authorship, and/or publication of this article.

#### References

- ABAQUS (2012) *Abaqus scripting user's manual*, 6.12-3. Dassault Systèmes Simulia Corp., Providence, RI.
- Belleri A, Schoettler MJ, Restrepo JJ, et al. (2014) Dynamic behavior of rocking and hybrid cantilever walls in a precast concrete building. *ACI Structural Journal* 111(3): 661–672.
- Belleri A, Torquati M and Riva P (2013) Finite element modeling of “rocking walls.” In: *4th ECCOMAS thematic conference on COMPDYN*, Kos Island, 12–14 June.
- Carr AJ (2004) *Ruamoko, Vol. 2: User Manual for the 2-Dimensional Version*. Christchurch, New Zealand: Department of Civil Engineering, University of Canterbury.
- Cheng CT (2007) Energy dissipation in rocking bridge piers under free vibration tests. *Earthquake Engineering & Structural Dynamics* 36(4): 503–518.
- Conley J, Sritharan S and Priestley MJN (2002) *Precast seismic structural systems PRESS-3: the five-story precast test building, vol. 3-1: wall direction response*. Report no. SSRP-99/19, July. La Jolla, CA: University of California, San Diego.
- Data repository (n.d.) Available at: <https://nees.org/warehouse/experiment/918/project/46>

- Housner GW (1963) The behavior of inverted pendulum structures during earthquakes. *Bulletin of the Seismological Society of America* 53(2): 403–417.
- Kurama Y (2002) Hybrid post-tensioned precast concrete walls for use in seismic regions. *PCI Journal* 47(5): 36–59.
- Ma QTM (2010) *The mechanics of rocking structures subjected to ground motion*. PhD Thesis, Department of Civil and Environmental Engineering, University of Auckland, Auckland, New Zealand.
- Marriott D (2009) *The development of high-performance post-tensioned rocking systems for the seismic design of structures*. PhD Thesis, University of Canterbury, Christchurch, New Zealand.
- Marriott D, Pampanin S, Bull D, et al. (2008) Dynamic testing of precast, post-tensioned rocking walls systems with alternative dissipating solutions. *Bulletin of the New Zealand Society for Earthquake Engineering* 41(2): 90–103.
- Morgen BG and Kurama YC (2008) Seismic response evaluation of posttensioned precast concrete frames with friction dampers. *Journal of Structural Engineering* 134(1): 132–145.
- Muthukumar S and DesRoches R (2006) A Hertz contact model with non-linear damping for pounding simulation. *Earthquake Engineering & Structural Dynamics* 35(7): 811–828.
- Nasi KTJ (2011) *Stability of rocking structures*. MSCE Thesis, Purdue University, West Lafayette, IN.
- O'Hagan J, Twigden KM and Ma QT (2013) Sensitivity of post-tensioned concrete wall response to modelling of damping. In: *New Zealand society for earthquake engineering technical conference*, Wellington, New Zealand; Auckland, New Zealand 26–28 April, 2013.
- Pennucci D (2008) *Displacement based design of precast walls with additional dampers*. MSc Dissertation, European School for Advanced Studies in Reduction of Seismic Risk (ROSE School), University of Pavia, Pavia.
- Pollino M and Bruneau M (2007) *Analytical and experimental investigation of a controlled rocking approach for the seismic protection of bridge steel truss piers*. Technical report MCEER-08-0003. Buffalo, NY: Multidisciplinary Center for Earthquake Engineering Research, The State University of New York at Buffalo 21 January, 2008.
- Priestley MJN, Sritharan S, Conley J, et al. (1999) Preliminary results and conclusions from the PRESSS five-story precast concrete test building. *PCI Journal* 44(6): 42–67.
- Restrepo JI and Rahman A (2007) Seismic performance of self-centering structural walls incorporating energy dissipators. *Journal of Structural Engineering* 133(11): 1560–1570.
- Schoettler MJ (2010) *Seismic demands in precast concrete diaphragms*. PhD Thesis, Department of Structural Engineering, University of California, San Diego, La Jolla, CA.
- Schoettler MJ, Belleri A, Zhang D, et al. (2009) Preliminary results of the shake-table testing for the development of a diaphragm seismic design methodology. *PCI Journal* 54(1): 100–124.
- Smith BJ and Kurama YC (2012) *Seismic design guidelines for special hybrid precast concrete shear walls*. Report no. NDSE-2012-02, June. Notre Dame, IN: Department of Civil Engineering and Geological Sciences, University of Notre Dame.
- Spieth HA, Carr AJ, Murahidy AG, et al. (2004) *Modelling of post-tensioned precast reinforced concrete frame structures with rocking beam-column connections*. Research report no. 2004-X. Christchurch, New Zealand: Department of Civil Engineering, University of Canterbury.
- Toranzo LA (2002) *The use of rocking walls in confined masonry structures: a performance-based approach*. PhD Thesis, University of Canterbury, Christchurch, New Zealand.
- Wiebe L and Christopoulos C (2009) *Mitigation of higher mode effects in base-rocking systems by using multiple rocking sections*. Research report ROSE-2009/01. Pavia: IUSS Press.
- Wiebe L and Christopoulos C (2010) Characterizing acceleration spikes due to stiffness changes in nonlinear systems. *Earthquake Engineering & Structural Dynamics* 39(14): 1653–1670.